BOLLETTINO DI GEOFISICA TEORICA ED APPLICATA VOL. 45, N. 1-2, PP. 71-87; MAR.-JUN. 2004

Elastic moduli and seismogenic aspects of the Friuli upper crust

R. DE FRANCO[1], G. BRESSAN[2] and G.F. GENTILE[2]

[1] *Consiglio Nazionale delle Ricerche, Istituto per la Dinamica dei Processi Ambientali, Milano, Italy*
[2] *Istituto Nazionale di Oceanografia e di Geofisica Sperimentale - OGS, Trieste, Italy*

(Received December 18, 2002; accepted September 23, 2003)

Abstract - We investigated the correlation between the spatial pattern of the elastic moduli and the seismicity in the central part of the Friuli region, the most active seismic zone in north-eastern Italy. The bulk modulus, the shear modulus and the Poisson ratio are calculated from *Vp* and *Vp*/*Vs* tomographic images. Seismicity correlates best with the shear modulus. Among the parameter derivatives, the shear modulus Laplacian is the best correlated parameter, negatively related to the released seismic energy. The zones with negative Laplacian are characterized by spatial shear modulus variation concavity, suggesting that the seismogenic volume could be formed by two zones. One zone is characterized by competent rocks with a great capability of storing strain energy and is a strong potential for severe earthquakes. The other zone, surrounding the former, is composed of less competent rocks, with low strain energy and low seismic energy release. These results suggest that the spatial pattern of a shear modulus could be useful to investigate the seismogenic behaviour, particularly in areas affected by complex tectonics, where it is difficult to recognize seismically active faults.

1. Introduction

Earthquakes in the brittle regime are caused by a sudden rupture along shear planes, commonly referred to as faults. As shown by Cox and Scholz (1988), the geometry of faults is quite complex, consisting of arrays of shear fractures surrounded by zones affected by pervasive

Corresponding author: G. Bressan, Istituto Nazionale di Oceanografia e di Geofisica Sperimentale, Dip. C.R.S., Via Treviso, 55 - C.P. 1, Cussignacco (Udine), Italy; phone: +39 0432522433, fax: +39 043252247; e-mail: gbressan@inogs.it

fracturing. In most cases, the geometry of cracks and the texture of the relevant strained rocks is so complex and involves broad volumes that the term "fault zone" is preferred. Fault zones, composed of highly fractured rocks, fault gouges and fluids, are characterized by variations in geophysical properties (Eberhart-Phillips et al., 1995). Foxall et al. (1993) related fault zone velocity structure to fault zone mechanical properties. Eberhart-Phillips and Michael (1993) showed that the Parkfield region of the San Andreas Fault (SAF) is characterized by a high P-velocity variability. Thurber et al. (1997) found that the SAF in the Northern Gabilan range, central California, is characterized by a zone of low *Vp* and high *Vp*/*Vs* extending down to 6 km in depth. Michelini and Mc Evilly (1991) showed that the Parkfield fault zone is characterized by high *Vp*/*Vs* ratio. Li et al. (1994) showed that the fault zone of the 1992 Landers earthquake is characterized by a *Vs* 30 to 50 percent lower than that of the surrounding rock. Zhao and Mizuno (1999) proposed that high density cracks and high saturation rate, affecting the hypocenter zone of the Kobe earthquake (M_L 7.2), caused stress concentrations and the nucleation of the main shock.

The mechanical properties of the crust are very important for a better understanding of the seismogenic process and the recognition of seismically active fault zones. Heterogeneous mechanical properties of earthquake source zones are expected to produce variations in the elastic moduli patterns.

In this paper, the bulk modulus, Poisson ratio and the shear modulus are computed from 3-D *Vp* and *Vp*/*Vs* tomographic images and gravity modelling (Gentile et al., 2000) in the central part of the Friuli area (northeastern Italy). The patterns of the elastic moduli are compared with the seismicity in order to investigate the seismogenic characteristics of the central Friuli area, the most active seismic zone in the region.

2. Structural setting

The Friuli area is characterized by a complex tectonic pattern (Fig. 1a), resulting from the superposition of several Cenozoic-Age tectonic phases. The structural setting (Fig. 1b), according to Venturini (1991), consists mainly of two indented tectonic wedges, outlined by NE-SW and NW-SE orientated paleofault systems. The main tectonic lineaments are an E-W-trending system of S-verging thrusts and folds, with a few backthrusts and NW-SE-trending thrusts with SW vergence. These structures are intersected by strike-slip and normal faults, striking about NW-SE and NNE-SSW. The paleofault systems were characterized by strike-slip movements from Paleozoic to middle Eocene times and were re-activated during Cenozoic tectonic events. The main tectonic phases that affected the region were: the Mesoalpine NE-SW oriented compression (Middle-Late Eocene), the Neoalpine N-S oriented compression (Middle Miocene-Earliest Pliocene) and the Neoalpine NW-SE oriented compression (Pliocene).

The main pre-existing faults, inherited and then reactivated during these compressive events, fragmented the crust into different tectonic domains. The upper crust, in the central Friuli area, underwent a severe shortening and the Mesozoic cover was detached from the

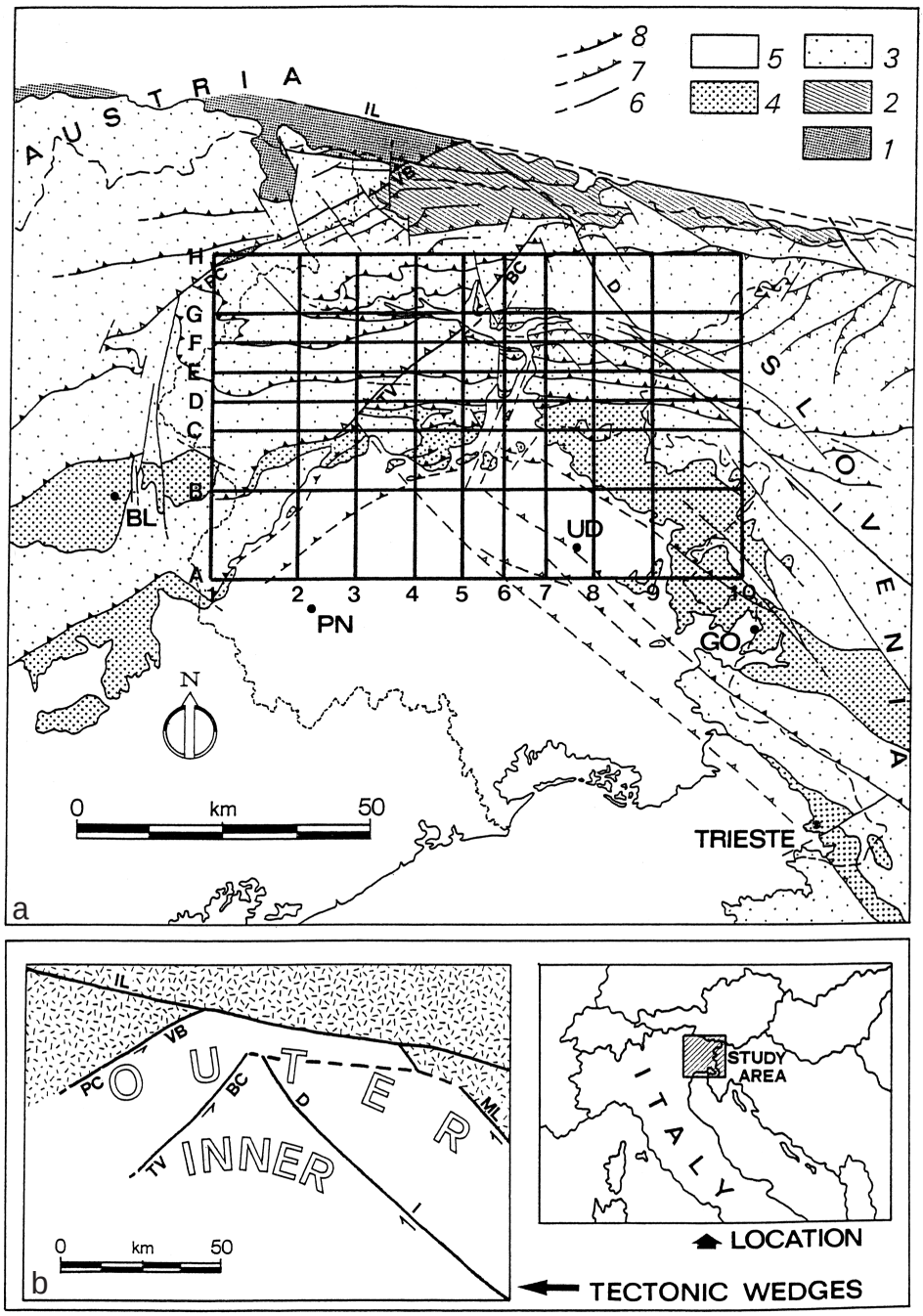

Fig. 1 - a) Schematic geologic map with the location of the tomographic grid: 1) Hercynian very-low metamorphic basement (Ordovician-Carboniferous); 2) Paleocarnic Chain, non-and anchimetamorphic succession (Upper Ordovician-Carboniferous); 3) Upper Carboniferous and Permo-Mesozoic carbonate successions; 4) Flysch (Upper Maastrichtian-Middle Eocene) and molassic sequence (Miocene); 5) Quaternary covers; 6) Subvertical fault; 7) Reverse fault, sometimes ancient syn-sedimentary fault reactivated as compressional fault; 8) Thrust. PC-VB: Pieve di Cadore and Val Bordaglia lines; TV-BC: Tramonti-Verzegnis and But-Chiarsò lines; D-I: Dogna and Idria lines; IL: eastern Insubric lineament (Gailtal line); ML: Mojstrana and Ljubljana lines. BL: Belluno town; PN: Pordenone town; UD: Udine town; GO: Gorizia town. b) The inset shows the two indented tectonic wedges as depicted by the faults described above, enhanced by capital letters and the location of the study area (from Bressan et al., 2003).

crystalline basement, which is located at a depth of nearly 10 km. This complex deformation pattern has been revealed by the 3-D *Vp* and *Vp*/*Vs* models of the upper crust, obtained through local earthquake tomography (Gentile et al., 2000). The upper crust is characterized by discontinuous blocks and bulges marked by strong lateral heterogeneity in *Vp* and *Vp*/*Vs* values. The tomographic images highlight a high-velocity body ($Vp \geq 6.2$ km/s) in the central part of the area, located at about a 6 km depth, bounded by sharp *Vp*/*Vs* variations.

The seismic activity (Fig. 2) is focused mainly on the central part of the study area which is affected by a compressional state of stress, with a sub-horizontal maximum compression axis, oriented from NNW-SSE to N-S (Bressan et al., 2003). This is where, the 1976-1977 sequence with a M_L 6.4 main shock (Barbano et al.,1985; Slejko et al., 1999) took place. The most important earthquake in north-eastern Italy in the last century. Maximum seismicity is located in

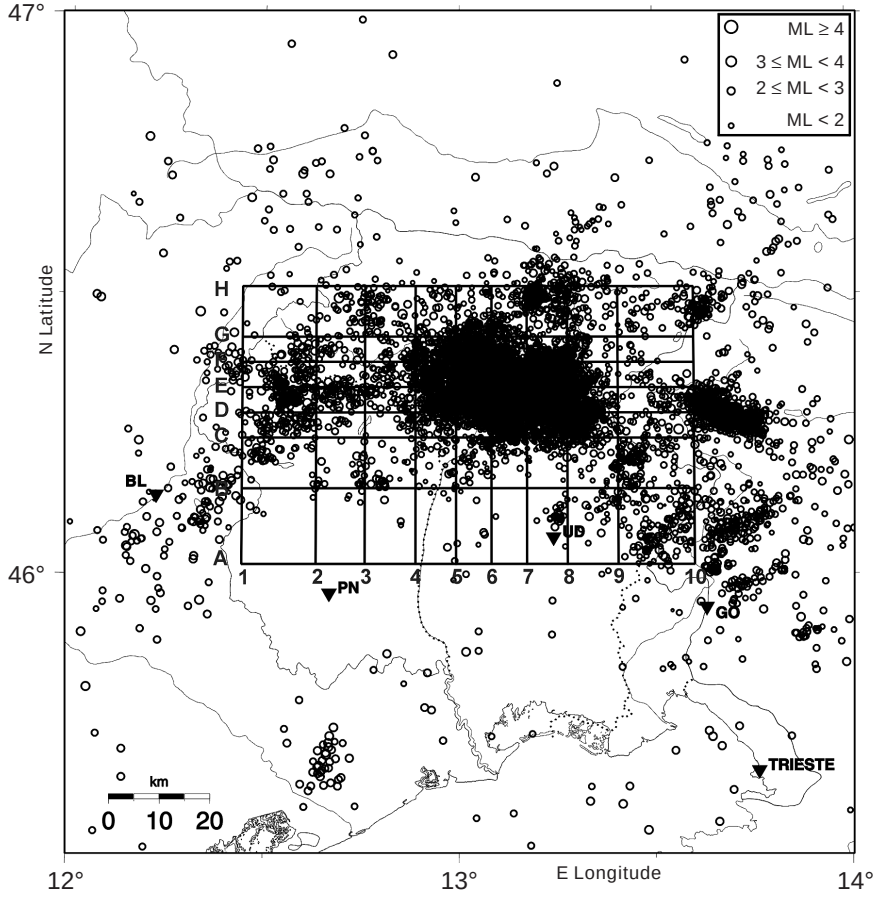

Fig. 2 - Map of the seismicity (circles) recorded from 1977-1999 by the INOGS local seismic array with the location of the 3-D *Vp* and 3-D *Vp*/*Vs* inversion grid (from Gentile et al., 2000). The size of circles are proportional to the local magnitude M_L, that varies from 1.0 to 5.6. Letters A to H mark south to north grid nodes. km distances are: -35(A), -20(B), -10(C), -5(D), 0(E), 5(F), 10(G), 20(H). Numbers 1 to 10 mark west to east grid nodes. km distances are: -50(1), -35(2), -25(3), -15(4), -7(5), 0(6), 7(7), 15(8), 25(9), 40(10). The depth spacing is 2 km from surface to 12 km. The vertical and horizontal errors location are less than or equal to 3 km. BL: Belluno town; PN: Pordenone town; UD: Udine town; GO: Gorizia town.

the depth range of 6-11 km. The depth distribution of seismicity suggests a brittle-ductile rheological transition located at about a 12 km depth (Bressan et al., 1992).

Earthquakes occur mainly or near the high-velocity body revealed by the tomographic images. The earthquakes appear to be located along the variation of the *Vp*/*Vs* anomalies. The main shocks of the 1976-1977 sequence are located at the southern border of the high-velocity bulge.

3. Elastic moduli

The tomographic images of *P* velocity and *P*-to *S*-velocity ratio (Gentile et al., 2000) were obtained initially by computing a reliable 3-D *Vp* model and then inverting for *Vp*/*Vs* values. This procedure may create biased *S* models, but it was recommended by Thurber (1993) and Eberhart-Phillips and Reyners (1997) in cases such as ours where the *S*-wave data are of poorer quality and fewer in number than the *P*-wave data. According to Thurber and Atree (1993), this approach has some advantages when variations in *Vp*/*Vs* are used to investigate the geological structure and mechanical properties. *Vp*/*Vs* models inferred from the direct inversion of the *S*-velocity model, when *S*-wave data are of poorer quality than the *P* data, are mainly controlled by the perturbation of *Vp*. Faithful images of significant *Vp*/*Vs* variations, instead, can be obtained from the direct inversion of 3-D *Vp*/*Vs* values.

The *Vp* and *Vs* values were interpolated on a horizontal grid mesh of 2.5 km x 2.5 km and 1 km in depth with the De Boor (1978) algorithm. The size of the grid mesh was chosen by considering the extent of the seismogenic structures. The rupture area radius of the earthquakes relocated with tomographic models, ranges from 0.15 to 0.5 km (Franceschina, personal communication) for a local magnitude ranging from 1.5 to 4.3. We recall that the estimated fault dimensions of the main shock of the 1976 sequence (M_L 6.4) were 13 x 13.8 km (Zollo et al., 1997). The *P*-wave velocities were then converted into densities using the velocity-density relationship by Zelt and Smith (1992). The validity of the density model, obtained with these relations, was previously verified (Gentile et al., 2000) on the cross-sections 5, 7 and E (Fig. 1) with a gravity inversion, minimizing the differences between computed Bouguer gravity anomalies and the observed ones. The inversion showed that the variations of the optimized density model affect only the superficial layers (2-4 km depth). The bulk modulus, the Poisson ratio and the shear modulus were then calculated using the relationships between elastic moduli and the values of density, *Vp* and *Vs*.

Figs. 3 and 4 show the calculated elastic moduli (shear modulus, Poisson ratio, bulk modulus) at 6 and 8 km depth slices, respectively. The location of the horizontal layers were selected considering the best spatial resolution of the velocity anomalies and the increase of the earthquake frequency at a 5-6 km depth (Bressan et al., 1992). The relations between the elastic moduli and the seismicity are investigated in the area where the *Vp* and *Vp*/*Vs* anomalies are best resolved.

According to the checkerboard and restore-resolution tests (Gentile et al., 2000), the *Vp* and *Vp*/*Vs* velocity anomalies are best resolved in the grid mesh area bounded by E-W – 40 + 20 km

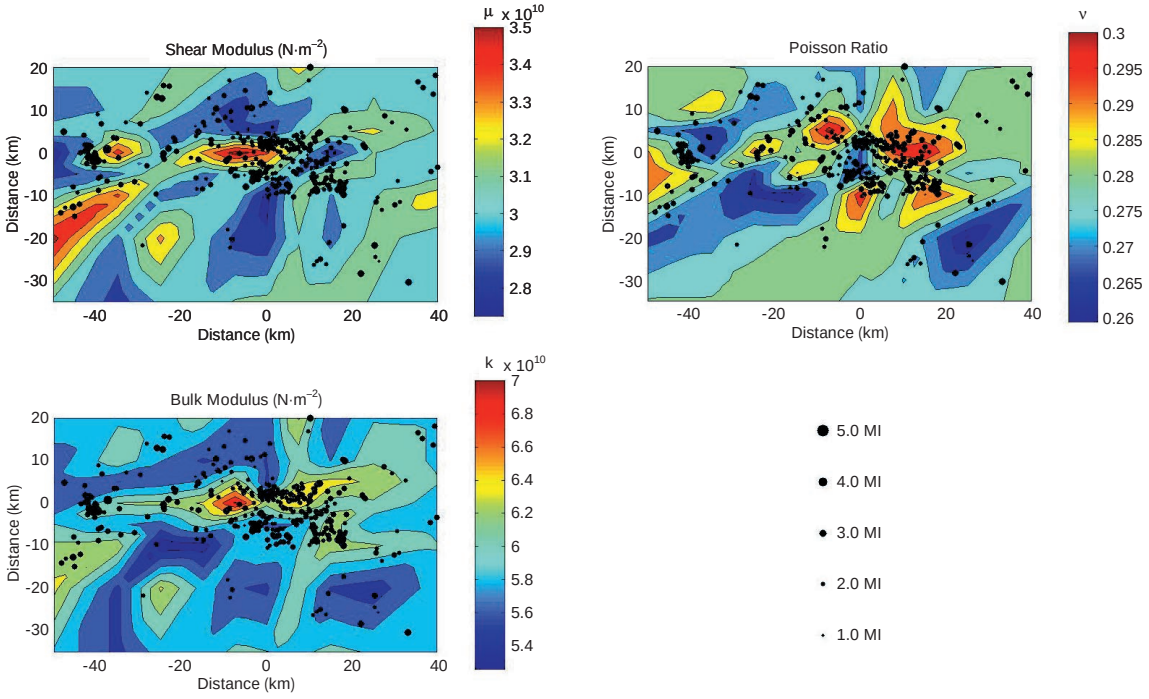

Fig. 3 - Elastic moduli (shear modulus, Poisson ratio, bulk modulus) calculated at 6 km depth slice, plotted in contour colours. The earthquakes are plotted as circles with size proportional to the local magnitude M_L, that varies from 1.5 to 4.3. The dimensions of the panels are the same as in the grid shown in Fig. 2.

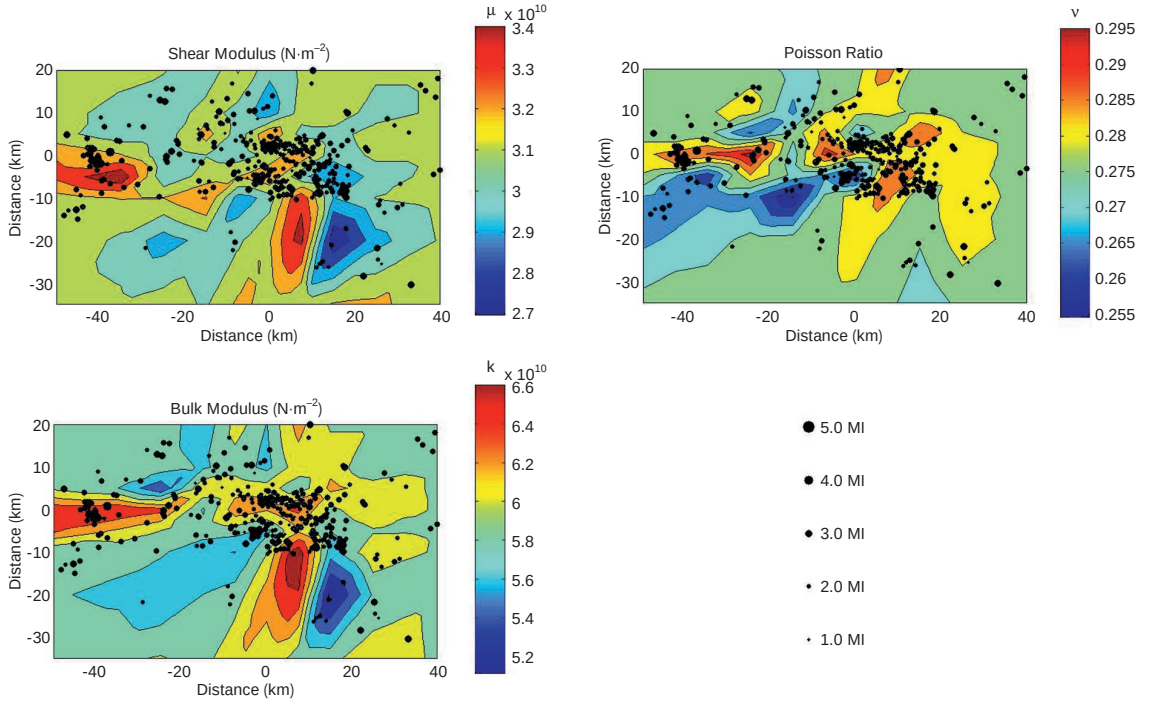

Fig. 4 - Elastic moduli (shear modulus, Poisson ratio, bulk modulus) calculated at 8 km depth slice, plotted in contour colours. The symbols of the earthquakes are the same of Fig. 3. The dimensions of the panels are the same as in the grid shown in Fig. 2.

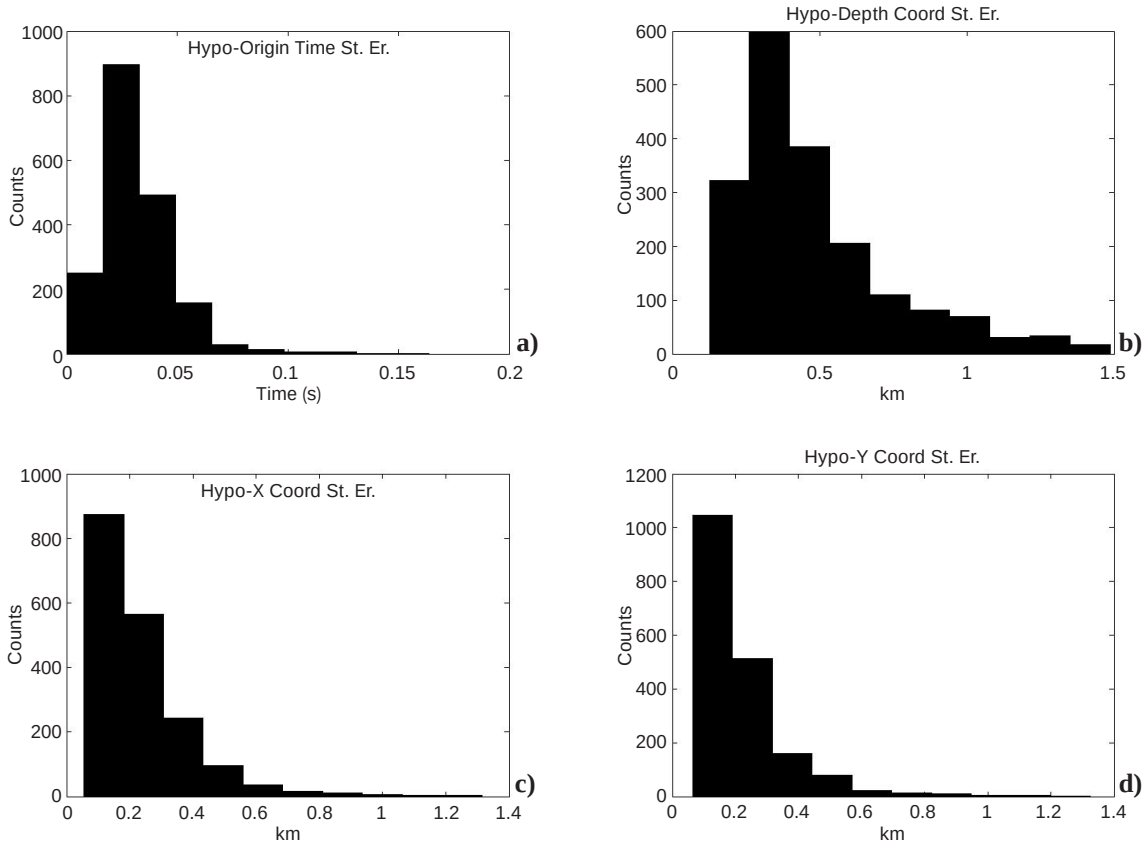

Fig. 5 - Histograms showing the hypocentral errors versus the number of the relocated earthquakes: a) standard errors relative to the origin time; b) standard errors relative to the depth; c) standard errors relative to X coordinates of the grid showed in Fig. 2; d) standard errors relative to Y coordinates of the grid showed in Fig. 2.

coordinates and by N-S – 15 + 10 km coordinates, from a 4 to 8 km depth. Artifacts in the elastic moduli could be produced from the 3-D *Vp* and *Vp*/*Vs* models. We calculated the mean of relative errors of the elastic moduli from the error propagation theory, considering the elastic moduli as indirect measures of *P*-velocity, *P*-to *S*-velocity ratio and density. The evaluated mean of relative errors are 5%, 4% and 6% for the shear modulus, Poisson ratio and bulk modulus, respectively.

A total number of 1897 events from 1988 to 1999 ($1.5 \leq M_L \leq 4.3$) were relocated using the *Vp* and *Vp*/*Vs* tomographic model. Fig. 5 shows the hypocentral errors. The mean of the standard errors relative to the time of origin (Fig. 5a) is 0.03 s (standard deviation of the errors 0.01 s), lower than the estimated picking error of the *P* and *S* arrival times used in the tomographic inversion of Gentile et al. (2000). The estimated picking accuracy of *P*-wave arrival times was ± 0.05 s. The picking accuracy of *S*-wave arrival times was ± 0.1 s and ± 0.15 s for 3-D seismometers and vertical seismometers, respectively. The mean of the standard errors relative to the hypocentral coordinates (Figs. 5b, 5c, 5d) are: 0.48 km (depth) with standard

deviation of the errors 0.27 km; 0.25 km (x coordinates) with standard deviation of the errors 0.15 km; 0.22 km (y coordinates) with standard deviation of the errors 0.14 km. The spatial location errors are less than the block dimensions used for the calculation of the earthquake density and the seismic energy released.

The model is parametrized by a grid mesh without boundaries or layer discontinuities. It must be recalled that the crust could be affected by seismic discontinuities not corresponding to geological boundaries and denoting some physical process, as shown by Lyakhovsky and Myasnikov (1987), who simulated the formation of discontinuities on the seismic properties of the rocks caused by a process of cracking induced by the tectonic stress.

4. Results and discussion

The shear modulus, the Poisson ratio and the bulk modulus (Figs. 3 and 4) are characterized by a complex pattern, reflecting the structural heterogeneity of the crust. As pointed out, this area corresponds to a poliphase deformational belt produced by the superposition of several tectonic phases, each characterized by different orientations of the principal axes of stress (Castellarin et al., 1992). The seismicity is grossly located where the shear modulus is low and in some cases along its sharp variations. A well-defined relation between the Poisson ratio and the bulk modulus images and the seismicity is not observed. In some parts, the seismicity seems

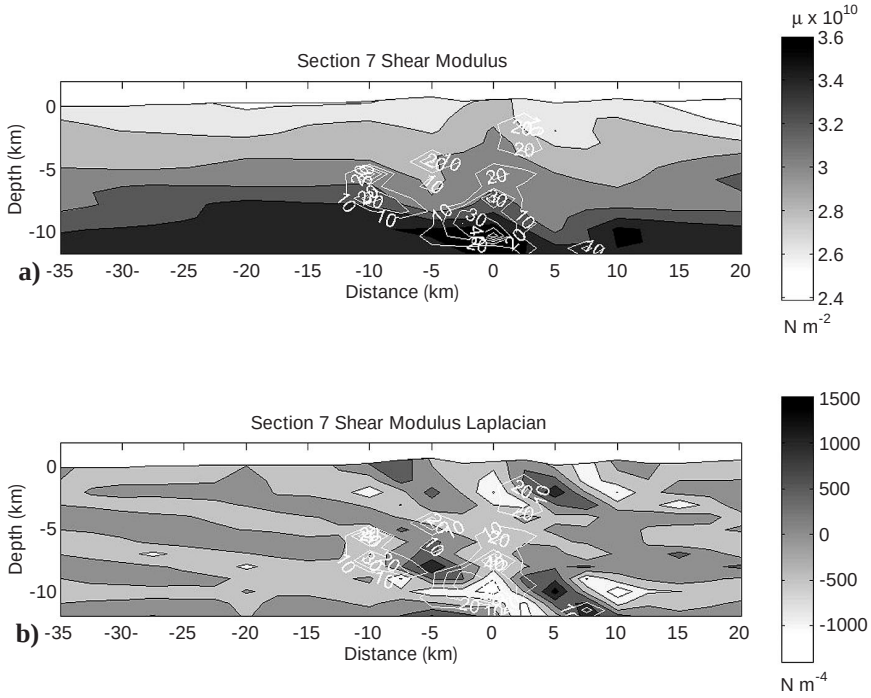

Fig. 6 - Shear modulus (a) calculated along vertical N-S cross-section n. 7 of Fig. 2 and shear modulus Laplacian (b), plotted in grey tones. The earthquake density is drawn in contour lines.

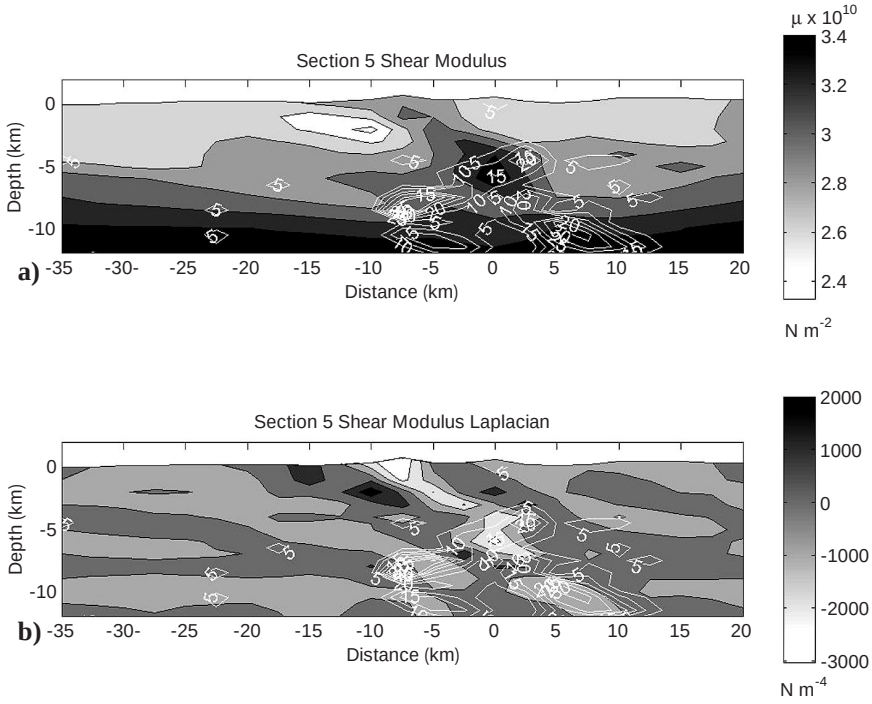

Fig. 7 - Shear modulus (a) and shear modulus Laplacian (b), in grey tones, calculated along vertical N-S cross-section n. 5 of Fig. 2, with the earthquake density (contour lines).

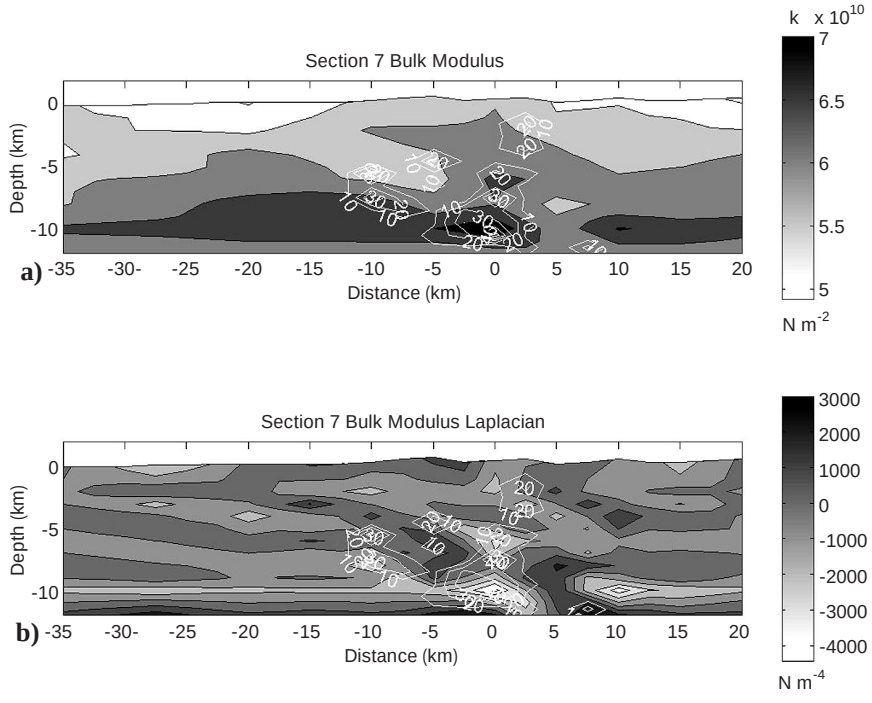

Fig. 8 - Bulk modulus (a) and bulk modulus Laplacian (b), in grey tones, calculated along vertical N-S cross-section n. 7 of Fig. 2, with the earthquake density (contour lines).

located along the sharp variations of these moduli, but a clear general trend is not recognizable. Figs. 6a and 7a show the shear modulus with the earthquake density for vertical cross-sections 7 and 5 (Fig. 2), respectively. The bulk modulus, calculated along vertical cross-section 7, with the earthquake density, is shown in Fig. 8a. The pattern of the elastic moduli is characterized by lateral variations in the area best resolved by the tomographic inversion. The high-velocity body revealed by the *Vp* and *Vp*/*Vs* images (Gentile et al., 2000) corresponds to the body with high shear modulus in section 5 (Fig. 7a).

The earthquake density ε was computed counting the number of earthquakes inside blocks the size of 2.5 x 2.5 x 1 km to investigate the correlation in the seismicity, the geophysical parameters (*Vp*, *Vs*, density ρ) and the calculated elastic moduli. The correlation coefficients within the geophysical parameters, elastic moduli and earthquake density, computed along vertical cross-sections 5 and 7, in the distance range between – 12.5 and 10 km along N-S coordinates and in the depth range 2.5 -10.5 km, corresponding to the area where the *Vp* and *Vp*/*Vs* models are best resolved, are shown in Table 1. The correlation coefficients are computed using the relation $C(i,j) / (C(i,i) \cdot C(j,j))^{1/2}$ where $C(i,j)$ is the covariance matrix.

Generally, the correlation coefficients are low, with the higher correlation coefficients related to *Vs* and shear modulus. Among the elastic moduli, the shear modulus is the best correlated parameter with the seismicity.

The relation between the seismicity and the mechanical properties of the fault zones is a controversial matter. For Thurber et al. (1997), most of the seismic activity in the SAF is associated to zones of high *Vp*/*Vs*. While studying the correlation between the *P*-velocity model and the induced seismicity in mines, Maxwell and Young (1992) observed that most of the events were located in a region near a high-velocity zone and (this is not a contradiction) predominantly concentrated in a zone of high-velocity gradient. Maxwell and Young (1992, 1995) provided an interpretation relating the velocity variation to the variation of the state of stress of a rock mass. A decrease of the state of stress reduces the shear strength/stiffness by reducing the normal stress across pre-existing crack surfaces, which allows cracks to open, and consequently results in a decrease in seismic velocity. Conversely, an increase of the stress state causes the normal stress, across pre-existing crack surfaces, to increase making cracks close, and, consequently, leading to an increase in seismic velocities. The high-velocity gradient, between high and low velocity zones, is mainly correlated to low-magnitude

Table 1 - Correlation coefficients of geophysical parameters (*Vp*: P-wave velocity, *Vs*: shear wave velocity), elastic moduli (ρ: density, *K*: bulk modulus, μ: shear modulus, ν: Poisson ratio) and earthquake density (ε), along vertical cross-sections 5 and 7.

Parameter *p*	**C (p, ε)**	**C ($\lvert\nabla p\rvert$,ε)**	**C ($\nabla^2 p$, ε)**
Vp	0.41	-0.006	-0.33
Vs	0.52	0.014	-0.41
ρ	0.30	0.1	-0.17
K	0.30	-0.05	-0.24
μ	0.54	0.02	-0.45
ν	-0.21	-0.22	0.08

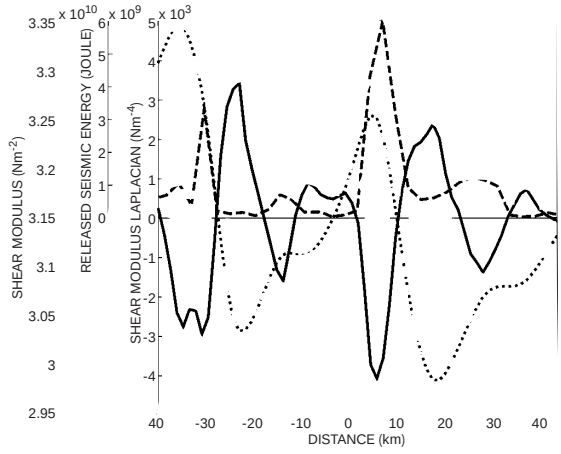

a)

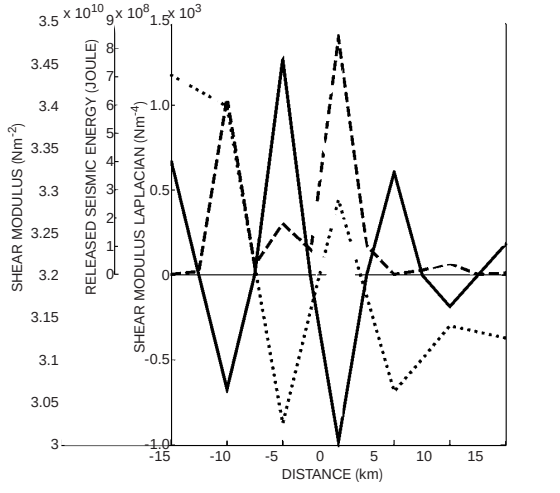

b)

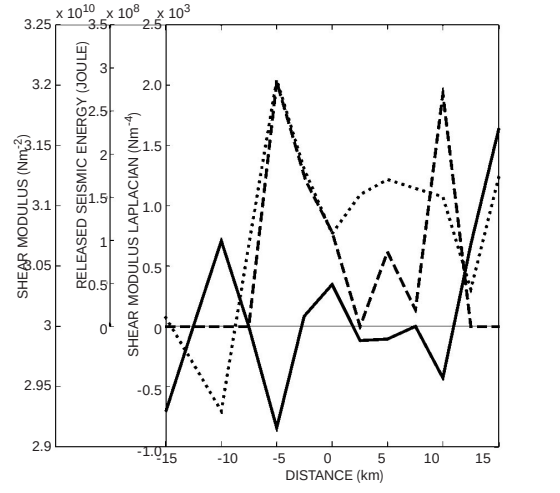

c)

Fig. 9 - Values of shear modulus (dotted), shear modulus Laplacian (solid) and released seismic energy (dashed) computed at 8 km depth, along cross-sections (Fig. 2): D, E-W oriented (a); 7, N-S oriented (b), 5, N-S oriented (c). The earthquakes selected for the seismic energy estimate are located in the range of ± 1 km in depth and ± 2.5 km in N-S direction along cross-section D and ± 1 km in depth and ± 3.0 km in E-W direction along cross-sections 5 and 7.

seismicity. The zones of highest *P*-wave seismic velocity, corresponding to highly stressed rocks, are capable of storing considerable strain energy. The high-velocity zones may be characterized by lower seismic activity, but a high energy release. For Maxwell and Young (1992), low velocities are zones of decreased stress state of the rocks that favours microseismic activity. Zhao and Kanamori (1993,1995) found that most earthquakes of the 1992 Landers and the 1994 Northridge, California sequences, occurred in zones with relatively high *P*-wave velocities. They interpreted these zones as more competent parts along the fault zone that have greater capability of storing strain energy. Vlahovic and Powell (2001) investigated the relationship between the distribution of earthquakes and the 3-D *Vp*/*Vs* structure in the New Madrid zone. They observed that the hypocentres appear to be located along the edges of a more competent crust or high-velocity zones, surrounded by zones characterized by low velocity.

Generalizing, there are two view points on earthquake source zones. Some researchers suggest that earthquakes are located mainly in the high-velocity zones of the fault, other researchers point out that the earthquake occurrence zones feature low-velocity, high *Vp*/*Vs* ratio and a high-velocity gradient.

We therefore calculated the correlation coefficients for the gradient modulus and the Laplacian of the analyzed parameters (Table 1). The parameter gradients are poorly correlated with the seismicity. The Laplacian of the shear velocity, shear modulus and the bulk modulus show a negative correlation with the earthquake density. Figs. 6b and 7b show the Laplacian of the shear modulus with the earthquake density, for vertical cross-sections 7 and 5, respectively. The Laplacian of the bulk modulus calculated along vertical cross-section 7 is shown in Fig. 8b. Among the parameter derivatives, the Laplacian of the shear modulus shows the highest correlation value. The negative correlation of the Laplacian of the shear modulus and the earthquake density implies that the earthquake density is high where the shear modulus diminishes around a maximum value (concave feature). Fig. 9 shows the values of shear modulus, the Laplacian shear modulus and the seismic energy released computed along cross-section D, E-W oriented (Fig. 2), section 7 and section 5. The seismic energy was calculated with the relation used by Suhadolc (1981). The correlation coefficients between the released seismic energy and shear modulus are 0.50 (cross-section D), 0.56 (cross-section 7) and 0.53 (cross-section 5). The correlation coefficients between the seismic energy released and Laplacian shear modulus are -0.59 (cross-section D), -0.59 (cross-section 7) and -0.50, (cross-section 5). The correlation observed between the negative Laplacian of the shear modulus and the released seismic energy suggests a phenomenological relation of the form: $k\nabla^2\mu = -E_s$, where μ is shear modulus, k is a constant and E_s is the seismic energy released in time unit and unit of volume. In this relation, k has the physical dimension of a diffusion coefficient ($l^2\ t^{-1}$).

The above-quoted interpretations (Maxwell and Young, 1992; Zhao and Kanamori, 1993,1995; Vlahovic and Powell, 2001) considered the correlation of seismicity with the absolute value or the gradient of the elastic parameters. The present work introduces the concept of spatial shear modulus variation concavity. Concave features of the shear modulus function include areas where the local and absolute maximum of the shear modulus are bordered by areas

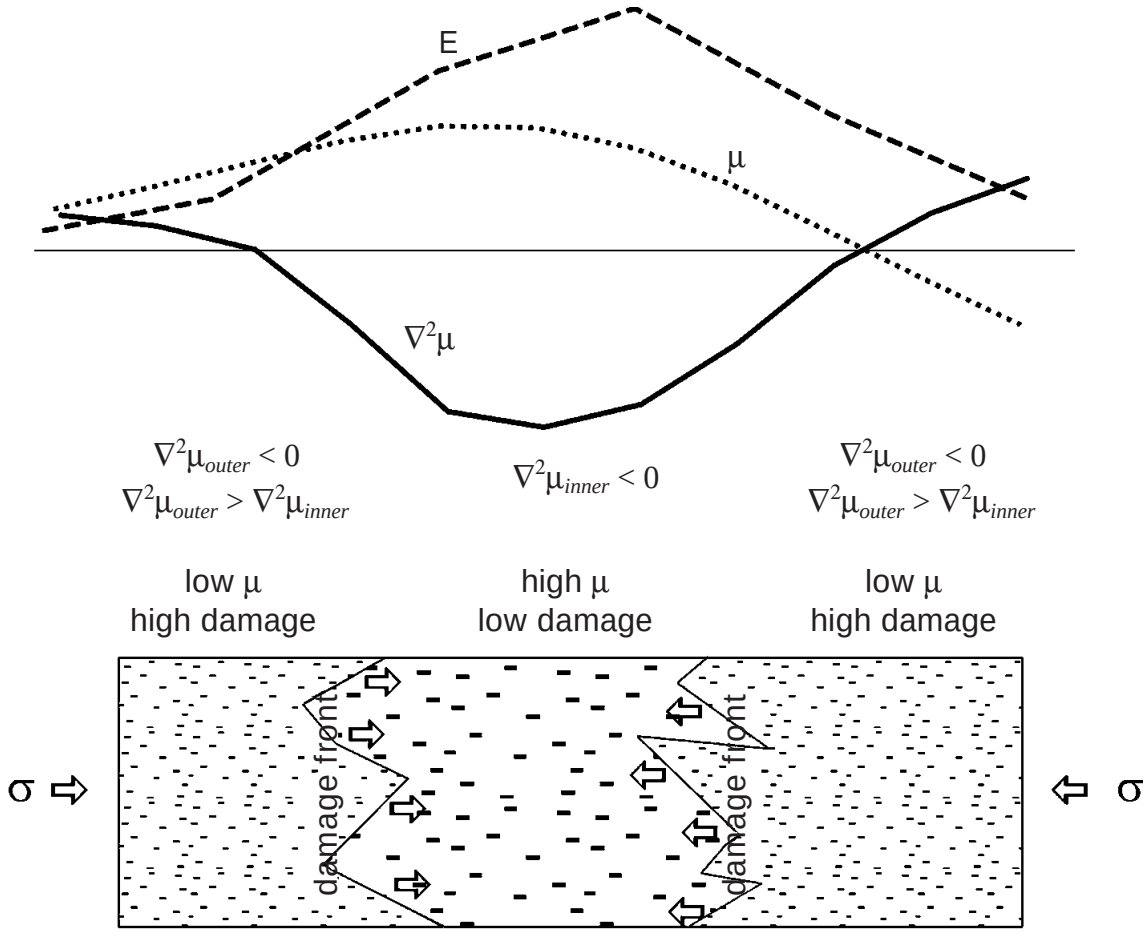

Fig. 10 - Cartoon showing the proposed model of an earthquake source zone. σ: tectonic stress, E: released seismic energy; μ: shear modulus, $\nabla^2\mu$: shear modulus Laplacian. The model consists of an inner zone characterized by high shear modulus, low damage and of outer zones characterized by low shear modulus, high damage. The shear modulus Laplacian of the inner zone is minor than that of the outer zones.

where it is reduced, and areas where the shear modulus, bordered by a monotonic increase in shear modulus flattens out or slightly decreases. All these areas correlate with seismicity, and we refer to them as shear modulus variation "concavity" or "concave features". The results of the present study suggest that most of the earthquakes are located in zones where the shear modulus variation shows a concave feature, also in areas where the shear modulus is characterized by relatively low values (interval distances between – 20 and – 10 km and between 20 and 30 km in Fig. 9a). Furthermore, the magnitude of the variation concavity correlates with the released seismic energy, that is, the zones with the highest variation concavity would be characterized by earthquake with the highest energy (Fig. 9).

According to the O'Connel and Budiansky (1974) model, the shear modulus is strongly dependent on the extent of the fracturing. Grady and Kipp (1987) defined the damage as a scalar parameter α, ranging between 0 and 1. $\alpha = 0$ corresponds to intact, undamaged rock and $\alpha = 1$

corresponds to complete failure. The damage parameter α may be seen as the density of cracks and fractures in a rock volume. So the damage α can be considered as the internal state variable which characterizes the state of fracturing. The damage reduces the intrinsic elastic modulus of the material B to a modulus B_f : $B_f = B\,(1 - \alpha)$. Ben-Zion et al. (1999) claimed that the effective elastic properties of rocks in the seismogenic zone are modified by the progressive damage caused by the ongoing deformation. Similar considerations were also made by Lyakhovsky et al. (1997), who assumed the shear modulus to be a function of the state of damage and, in their Eq. (35), they considered the derivative of the shear modulus with respect to time, as depending also on the evolution of the rate of damage. Therefore, the shear modulus can be considered as a function of the state of damage.

The concept of shear modulus variation concavity could synthesize the observations quoted in literature and the two main hypotheses regarding the earthquake source zones. The seismogenic volumes, characterized by shear modulus variation concavity (zones with negative Laplacian) appear to be formed by two zones (Fig. 10). An inner zone is characterized by more competent rocks (relative high-shear modulus, low damage and maximum negative Laplacian shear modulus), where high-strain energy can be stored and where major earthquakes occur. The surrounding (outer) zone is characterized by less competent rocks, with relativly low-shear modulus, high damage, and where more frequent, low-seismic energy events occur. The spatial extent of the inner zone depends on the magnitude of the shear modulus variation concavity. According to this model, the damage should propagate from relatively high-damage zones to low-damage zones and it varies with time. Therefore, the observed relation $k\nabla^2\mu = -E_s$ of the present work can be expressed in a more general form: $C\nabla^2\mu = \frac{\partial\mu}{\partial t}$, where C is a diffusion coefficient and $\frac{\partial\mu}{\partial t}$ represents the temporal variation of the shear modulus with the ongoing damage. In this case, $\frac{\partial\mu}{\partial t}$ accounts not only for the observed released seismic energy by brittle failure, but also for the overall deformation that progressively changes the structure of a rock.

5. Conclusions

The pattern of the elastic moduli (shear modulus, bulk modulus, and Poisson ratio) of the Friuli upper crust is complex and appears to be related to geologic-structural heterogeneity. From the elastic moduli, the shear modulus correlates best with the earthquake source zones. The gradients of the elastic moduli are poorly correlated with seismicity. From the parameter derivatives, the Laplacian shear modulus correlates best with the seismicity. The negative correlation of the Laplacian shear modulus with the seismicity indicates that the seismogenic volumes are characterized by spatial shear modulus variation concavity. The shear modulus can be considered as a function of the state of damage of a rock, that is the density of cracks and fractures. In the model proposed, the spatial variation concavity of the shear modulus is associated with two zones. An inner zone features a relative, high-shear modulus, low damage and is characterized by high-strain energy. The outer, surrounding zone, is characterized by a relative, low-shear modulus, high damage, with more frequent seismicity, but a low release of

seismic energy. Undoubtely, the model proposed in the present study needs further validations, for example by increasing the spatial resolution of 3-D *Vp*, *Vs* and density models and therefore of the elastic moduli pattern, which at present represents the main limitation of this investigation. However, even if the elastic moduli pattern does not give an exaustive definition of the rheological status of the crust, the Laplacian shear modulus could be an appropriate indicator of the earthquake source areas. This approach can be important especially in areas, like Friuli, characterized by the superposition of several strain patterns where the deep fault geometry is hardly inferable, and where it is difficult to recognize which segments or parts of the faults are seismically active.

Acknowledgments. The local seismic network is managed by the Dip. Centro Ricerche Sismologiche of the Istituto Nazionale di Oceanografia e di Geofisica Sperimentale with financial support from the Regione Friuli-Venezia Giulia. Thanks are due to David Zuliani and Sandro Urban for help in the graphics. We are greatful to A. Marcellini for helpful discussions and his encouragement.

References

Barbano M.S., Kind R. and Zonno G.; 1985: *Focal parameters of some Friuli earthquakes (1976-1979) using complete theoretical seismograms.* J. Geophys., **58**, 175-182.

Ben-Zion Y., Dahmen K., Lyakhovsky V., Ertas D. and Agnon A.; 1999: *Self-driven mode switching of earthquake activity on a fault system.* Earth and Planetary Science Letters, **172**, 11-21.

Bressan G., Bragato P.L. and Venturini C.; 2003: *Stress and strain tensors based on focal mechanisms in the seismotectonic framework of the Friuli-Venezia Giulia region (Northeastern Italy).* Bull. Seism. Soc. Am., **93**, 1280-1297.

Bressan G., De Franco R. and Gentile G.F.; 1992: *Active faulting and seismogenic aspects of the Friuli area.* Studi Geologici Camerti, **2**, CROP1-1A, 88-98.

Castellarin A., Cantelli L., Fesce A.M., Mercier J.L., Picotti V., Pini G.A., Prosser G. and Selli L.; 1992: *Alpine compressional tectonics in the Southern Alps. Relationship with the N-Apennines*. Annales Tectonicae, **6**, 62-94.

Cox S.J.D. and Scholz C.H.; 1988: *On the formation and growth of faults: an experimental study*. Journ. Struct. Geol., **10**, 413-430.

De Boor C.; 1978: *A practical guide to splines.* Springer-Verlag.

Eberhart-Phillips D.; 1990: *Three-dimensional P and S velocity structure in the Coalinga region, California.* Journ. Geophys. Res., **95**, 15,343-15,363.

Eberhart-Phillips D. and Michael A.J.; 1993: *Three-dimensional velocity structure, seismicity and fault structure in the Parkfield Region, Central California.* Journ. Geophys. Res., **98**, 15,737-15,758.

Eberhart-Phillips D. and Reyners M.; 1997: *Continental subduction and three-dimensional crustal structure: the Northern South Island, New Zealand.* Journ. Geophys. Res., **100**, 12,919-12,936.

Eberhart-Phillips D., Stanley W.D., Rodriguez B.D. and Lutter W.J.; 1995: *Surface seismic and electrical methods to detect fluids related to faulting.* Journ. Geophys. Res., **102**, 11,843-11,861.

Foxall W., Michelini A. and McEvilly T.V.; 1993: *Earthquake travel time tomography of the southern Santa Cruz Mountains: control of fault rupture by lithological heterogeneity of the San Andreas Fault zone.* Journ. Geophys. Res., **98**, 17,691-17,710.

Gentile G.F., Bressan G., Burlini L. and de Franco R.; 2000: *Three-dimensional Vp and Vp/Vs models of the upper crust in the Friuli area (northeastern Italy).* Geophys. J. Int., **141**, 457-478.

Grady D.E. and Kipp M.E.; 1987: *Dynamic rock fragmentation.* In: Atkinson B.K. (ed), Fracture mechanics of rock, Academic Press, pp. 429-475.

Li Y.G., Vidale J.E., Aki K., Marone C.J. and Lee W.K.; 1994: *Fine structure of the Landers fault zone: segmentation and the rupture process.* Science, **265**, 367-370.

Lyakhovsky V., Ben-Zion Y. and Agnon A.; 1997: *Distributed damage, faulting and friction.* Journ. Geophys. Res., **102**, 27,635-27,649.

Lyakhovsky V.A. and Myasnikov V.P.; 1987: *On the relation between seismic wave velocity and stress in a solid.* Geophys. J.R. Astr. Soc., **91**, 429-437.

Maxwell S.C. and Young R.P.; 1992: *Sequential velocity imaging and microseismic monitoring of mining-induced stress change.* Pageoph. **139**, 421-447.

Maxwell S.C. and Young R.P.; 1995: *A controlled in-situ investigation of the relationship between stress, velocity and induced seismicity.* Geophys. Res. Lett., **22**, 1049-1052.

Michelini A. and McEvilly T.V.; 1991: *Seismological studies at Parkfield. I. Simultaneous inversion for velocity structure and hypocenters using cubic b-splines parametrization.* Bull. Seism. Soc. Am., **81**, 524-552.

O'Connell R.J. and Budiansky B.; 1974: *Seismic velocities in dry and saturated cracked solids.* Journ. Geophys. Res., **35**, 5412-5426.

Slejko D., Neri G., Orozova I., Renner G. and Wyss M.; 1999: *Stress field (NE Italy) from fault plane solutions of activity following the 1976 main shock.* Bull. Seism. Soc. Am., **89**, 1037-1052.

Suhadolc P.; 1981: *Spatial distribution of the aftershock sequence relative to the September 16, 1977 Friuli earthquake.* Boll. Geof. Teor. Appl., **13**, 331-348.

Thurber C.H.; 1993: *Local earthquake tomography: velocities and Vp/Vs - theory.* In: Iyier H.M. and Hirahara K. (eds), Seismic tomography - theory and practice, Chapman and Hall, pp. 563-583.

Thurber C.H. and Atre S.R.; 1993: *Three-dimensional Vp/Vs variations along the Loma Prieta rupture zone.* Bull. Seism. Soc. Am., **83**, 717-736.

Thurber C., Roecker S., Ellsworth W., Chen Y., Lutter W. and Sessions R.; 1997: *Two dimensional seismic image of the San Andreas fault in the Northern Gablilan range, central California: evidence for fluids in the fault zone.* Geophys. Res. Lett., **24**, 1591-1594.

Venturini C.; 1991: *Cinematica neogenico-quaternaria del Sudalpino orientale (settore friulano).* Studi Geol. Camerti, Vol. Spec., 109-116.

Vlahovic G. and Powell C.A.; 2001: *Three-dimensional S wave velocity structure and Vp/Vs ratios in the New Madrid Seismic zone.* Journ. Geophys. Res., **106**, 13,501-13,513.

Zelt C.A. and Smith R.B.; 1992: *Seismic traveltime inversion for 2-D crustal velocity structure.* Geophys. J. Int., **108**, 16-34.

Zhao D. and Kanamori H.; 1993: *The 1992 Landers earthquake sequence: earthquake occurrence and structural heterogeneities.* Geophys. Res. Lett., **20**, 1083-1086.

Zhao D. and Kanamori H.; 1995: *The 1994 Northridge earthquake: 3-D crustal structure in the rupture zone and its relation to the aftershock location and mechanisms.* Geophys. Res. Lett., **22**, 763-766.

Zhao D. and Mizuno T.; 1999: *Crack density and saturation rate in the 1995 Kobe earthquake region.* Geophys. Res. Lett., **26**, 3213-3216.

Zollo A., Bobbio A., Emolo A. and Herrero A.; 1997: *Modelling of ground acceleration in the near source range: the case of 1976, Friuli earthquake (M=6.5), northern Italy.* Journ. of Seism., **1**, 305-319.